

Influence of Start-Up Time on the Purging of Salt Water From a Cavity by an Overflow of Fresh Water

N. Gillam¹, M.P. Kirkpatrick² and S.W. Armfield³

^{1,2,3}School of Aerospace, Mechanical and Mechatronic Engineering
The University of Sydney, Sydney, NSW, 2006 AUSTRALIA

Abstract

This paper presents the results of a numerical investigation of a flow in which salt water is purged from a square cavity by an overflow of fresh water. Ramp inlet velocity boundary conditions are used in order to describe the influence of the start up time on the amount of saline water purged from the cavity in the initial splash. As the time to start-up is increased, the volume of saline liquid purged from the pool is decreased. This has important implications in the management of river systems and the potential to purge the saline water within the river base by an environmental release, where it is expected that the time to start-up is measured in days.

Introduction

Density stratified turbulent mixing and transport is an important aspect of many industrial and geophysical flows. The purging of density stabilised basins by an overflow of fresh water is an aspect of density stratified mixing significant to the understanding of environmental release schemes and their associated success in the flushing of highly saline groundwater from the base of rivers within Australia and internationally. Salinisation of Australia's rivers is a direct result of the increase in groundwater recharge following the clearing of native vegetation for cropping or grazing since European settlement [12]. During times of low or zero flow, the saline pools are recharged primarily by groundwater intrusion through the riverbed. The pools generally consist of an upper layer of fresh water and a lower layer of saline water, typically contained within the scour holes at the base of the river and generally on river bends. The saline water within these pools is often of very poor quality, with low levels of dissolved oxygen (hypoxic) and salinities exceeding 50 000 ECS (34 000 ppm) in some parts. The saline pools render the base of the river uninhabitable for fish and other aerobic organisms [1], which would normally depend on these scour pools for breeding grounds and feeding.

During times of sufficiently large flow in the river, for example, as a result of heavy rainfall or an environmental release from managed and collected sources upstream, the overflow is capable of purging the pool of the saline water. The speed of the purging process is controlled by the rate at which the dense saline liquid is transported against a downward buoyancy force into the fresh water flowing above. Understanding the rates of purging under various conditions is of particular interest to catchment and river management teams, who must have a solid understanding of the environmental benefits or consequences of the environmental release, and plan release regimes accordingly. The scarcity of water for environmental flows means that the maximum purging of the saline groundwater from the pools must be achieved with the minimum volume of water. So-called 'black-water' events are of concern when mixing large quantities of the hypoxic and

highly saline ground water into the relatively fresh overflowing water, and the location and concentration of the purged saline water must be tracked in order to prevent possible fish kills. End-of-stream salinity targets must also be met.

Previous authors [2, 9] concentrated simulation and experimental efforts on instantaneous start-ups. However, in the current Australian drought, it is extremely unlikely that an environmental release would result in such favourable conditions. Transmission losses can reach as high as 80 percent [7], as patches of dry channel prior to the release must be filled before the flow will continue down the river. Thus, modelling must take this start-up time into account when deriving purging scale relationships, as it is anticipated that the time to start up in real life river applications is in the order of days.

This paper examines the influence of the start-up time on the amount of saline water purged during the initial splash, which was found [2] to produce a time rate of efflux two orders of magnitude greater than any other feature of the flow and is a result of the impulsive start-up of the flow. By removing this impulsive start-up, the magnitude of the drop in interface height and the volume of the dense saline fluid purged are compared against the start-up time.

The Purging Process

Previously, Armfield and Debler [2], performed experimental studies in a straight channel with a square cavity and numerically simulated this experiment with a 2D Direct Numerical Simulation (DNS) using a finite volume unsteady Navier-Stokes code. They found that the purging process could be characterised in terms of the Reynolds number of the overflow and the Rayleigh number based on the initial density variation.

The purging process of the pool has been categorised into 4 main stages:

1. The overflow initially pushes a large splash of the dense cavity liquid out of the cavity;
2. Vorticity generated from the upstream corner of the cavity forms a vortex which pulls lighter fluid into the cavity and mixes it with the denser fluid there, with an accompanying secondary splash;
3. A continuing seiche in the cavity ejects fluid from the resulting intermediate density layer;
4. The development of a circulatory motion in the upper portion of the cavity slowly transports the denser liquid below it by turbulent transport and molecular diffusion.

Stages 1-3 occur very rapidly, whereas Stage 4 typically takes 10 times as long.

The initial splash (Stage 1) was found to contribute by far the largest component to the time rate of transport of dense fluid

from the cavity into the duct, and that this initial splash was associated with the impulsive start-up.

Immediately after start-up and away from the inlet, the fluid responds inviscidly. The velocity field in the cavity is that of potential flow, with a line source at the entrance and a sink at the exit. The short-lived feature carries a substantial amount of dense fluid out of the cavity, removing twice as much saline fluid as any other feature of the flow, resulting in a sudden lowering of the interface. For the same geometry, the final height of the interface after this initial splash has passed decreases as the Froude number decreases [2]. The profile of the initial splash for all ramp times is included in the appendix.

Subsequent laboratory work [5] examined different cavity geometries, to include both rectangular and trapezoidal cavity shapes in order to determine the influence of the cavity shape on the rate and mode of mixing. By accelerating the flow sufficiently slowly in the channel, they found that the initial splash could be suppressed, although the interface did tilt slightly. This paper extends this finding, in order to determine the condition on the time to start-up that will suppress this initial splash.

The numerical simulations presented in this paper are performed on a 2-Dimensional (2D) Finite-Volume DNS code on a non-staggered grid. Although the 2D DNS simulation accurately predicts the initial wave and seiching, once these large-scale flow features have passed, the purging rate is dominated by breaking waves on the interface which eject streamers that are approximately 1 mm thick. These streamers cannot be captured on a computationally feasible grid and thus, the DNS code substantially under-predicts the purging rate during this part of the process. Only the initial wave and seiching are examined in this paper, as it is known that once breaking waves appear on the interface, the simulation accuracy diverges. A 3D simulation incorporating a Large Eddy Simulation (LES) turbulence model that permits backscatter would be required to accurately predict the later stages of purging [9], which is beyond the scope of this paper.

The Numerical Method

Governing Equations

The governing equations are the 2-D Navier-Stokes equations (1-3) and the solute transport equation (4), for an incompressible Boussinesq fluid in non-dimensional form in Cartesian coordinates as follows:

$$U_t + UU_x + VU_y = -P_x + \frac{1}{\text{Re}}(U_{xx} + U_{yy}), \quad (1)$$

$$V_t + UV_x + VV_y = -P_y + \frac{1}{\text{Re}}(V_{xx} + V_{yy}) - \frac{Ra\sigma}{\text{Pr Re}^2}, \quad (2)$$

$$U_x + V_y = 0, \quad (3)$$

$$\sigma_t + U\sigma_x + V\sigma_y = \frac{1}{\text{Re Pr}}(\sigma_{xx} + \sigma_{yy}). \quad (4)$$

Here the subscript indicates partial differentiation and U and V represent the non-dimensional velocity in the x and y directions respectively, P is the non-dimensional pressure, and σ is the non-dimensional solute concentration.

Dimensional Quantities

The length is non-dimensionalised by the length of the channel, L, the velocity by V_∞ , time by V_∞/L and pressure by ρV_∞^2 . To relate the solute concentration, σ , to the density ρ , the relation $\rho = \rho_{\text{water}} + \sigma$ is used, where the solute concentration is non-dimensionalised by $\sigma_{\text{cavity}} - \sigma_{\text{duct}}$.

The non-dimensional parameters used to define the flow are the Reynolds number and the Rayleigh number;

$$\text{Re} = \frac{V_\infty L}{\nu}; \quad \text{Ra} = \frac{gL^3 \Delta\rho}{\nu \kappa}; \quad (5)$$

where $\Delta\rho = (\rho_s - \rho_f)/\rho_f$ is the initial density differential and ρ_s and ρ_f are the initial densities of the salt (cavity) and fresh (duct) water respectively.

A densimetric Froude number may also be defined:

$$\text{Fr} = \left(\frac{\text{Re}^2 \text{Pr}}{\text{Ra}(H_{\text{cav}}/L)} \right) \quad (6)$$

The non-dimensional parameters chosen are:

$\text{Re} = 100\,000$; $\text{Ra} = 3.75 \times 10^{13}$; $\text{Pr} = 750$ (for salt), and the corresponding Froude number is 1.41.

These parameters lead to dimensional constants:

$u = 0.1 \text{ m/s}$ (free-surface velocity)
 $\Delta\rho = 0.005$ for $\rho_f = 1000 \text{ kg/m}^3$ & $\rho_s = 1005 \text{ kg/m}^3$
 $H_{\text{chan}} = 0.1 \text{ m}$
 $H_{\text{cav}} = 0.1 \text{ m}$
 $\nu = 1.0 \times 10^{-6} \text{ m}^2/\text{s}$ (Kinematic viscosity of water)
 $\kappa = 1.33 \times 10^{-9} \text{ m}^2/\text{s}$ (Kinematic diffusion coefficient for salt)

The Grid / Domain / Cavity

The domain is a duct of dimensional length 1m, with a channel height of 0.1m, which corresponds to the geometry used in [2, 9]. The cavity has an aspect ratio equal to 1.0 (Figure 1).

The equations of motion are discretised in space using a finite volume formulation on a non-uniform, non-staggered, Cartesian grid. The non-uniform grid permits the greatest resolution in the boundary layer regions and at the cavity – duct interface. The 2D grid has 130 x 130 cells in the x and y directions, with 30 x 80 cells concentrated in the cavity. Regions below the duct to the left and right of the cavity are masked.

The finite volume boundary condition means no nodes lie on the boundaries. Boundary conditions are implemented using ghost nodes placed outside the boundary. Ghost node values are then found by linear interpolation.

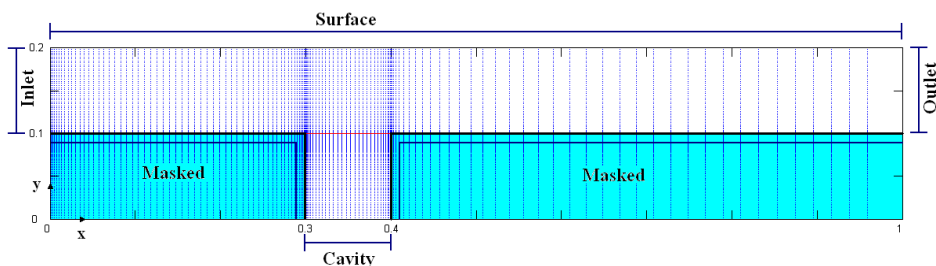


Figure 1. Computational Domain

Discretisation

All diffusion terms are approximated by second-order central differences as:

$$U_{xx}(x_i, y_j) = \left(\frac{U_{i+1} - U_i}{\Delta x_{i+1}} - \frac{U_i - U_{i-1}}{\Delta x_i} \right)_j + \left(\frac{\Delta x_{i+1} + \Delta x_i}{2} \right)_j + O(\Delta x^2) = SDU_{i,j} \quad (7)$$

Where SD is a finite difference operator, and $\Delta x_i = x_i - x_{i-1}$. The notation uses the index i to indicate the direction in the x direction and j indicates the y direction.

Previous authors [2,8] have shown that the used of a conventional 3rd order upwinding scheme, such as QUICK [10], resulted in oscillations on the interface, which resulted in unphysical non-dimensional solute concentrations, i.e. < 0 and > -1 . This was attributed primarily to the high flow to grid skewness present in the flow as the interface becomes distorted. These oscillations have been minimised by adopting the well-known modification of the QUICK scheme, SHARP [11]. The SHARP scheme is implemented on all derivatives occurring in convective terms

The Simple High-Accuracy Resolution Program (SHARP) adopts a criterion for monotonic resolution of the convective flux by normalising the convected control volume face value as a function of the normalised adjacent upstream node value. SHARP is based on an explicit, conservative, control volume flux formulation. The advantage of the SHARP scheme is that the standard QUICK algorithm (or a slight variation thereof) is used throughout the bulk of the flow domain while only thin regions requiring specialist treatment, such as thin shear layers and species density jumps. The advantages of the robustness of the QUICK scheme are maintained when using the SHARP scheme, and by only using the more complicated scheme where necessary, the SHARP scheme also maintains the time efficiency of the QUICK scheme.

Time Integration

The equations are solved in a segregated manner using a fractional step method on a non-staggered grid. The equations are integrated in time using a Crank-Nicolson time-stepping scheme for the diffusive terms and an Adams-Bashforth time stepping scheme for the advective terms. This method has been shown to be second order accurate in time [3], and is computationally efficient, as the momentum and pressure equations need only to be solved once every time-step.

The discretised momentum equations are written:

$$\frac{u^* - u^n}{\Delta t} + \frac{3}{2}H^n(u^n) - \frac{1}{2}H^{n-1}(u^{n-1}) = -G_x(p^n) + \frac{1}{2\text{Re}}L(u^* + u^n) \quad (11)$$

Here H is the advection operator, G the discrete gradient, L the discrete Laplace operator, and u^* the initial estimate of the velocity field. The superscript indicates the time step.

The momentum equations are first solved for the velocity, using the pressure field from the previous time step to find an approximate velocity field. A Poisson equation for the pressure correction is then solved. The pressure correction step enforces mass conservation and is used to correct the pressure field and project the approximate velocity solution onto a subset of divergence-free velocity fields. Thus, velocity and pressure fields satisfy both conservation of mass and momentum.

The equations are solved with a Bi-Conjugate Gradient Stabilised solver with preconditioning to increase the rate of convergence. The residuals were 1×10^{-5} for mass, 1×10^{-5} for momentum and solute concentration, and 1×10^{-7} for the pressure correction field.

Boundary Conditions

A parabolic $1/7^{\text{th}}$ power-law velocity profile is specified at the inlet with a zero salt concentration, while the outlet uses a zero-normal gradient outflow boundary condition for velocity and salt concentration. The free surface is modelled as a zero shear surface while the base of the duct is a no-slip surface. The solute boundary conditions are zero normal gradients at the surface, base and outlet. The normal derivative of the pressure correction is set to zero everywhere on the boundary. The pressure is obtained from the pressure correction at all internal points, and values on the boundary are obtained using a second order extrapolation from the interior points.

Initially, the fluid is at rest everywhere and the fluid in the duct, which represents the fresh water, has a solute concentration of 0, while in the cavity the solute concentration is set to 1. The solute concentration is diffused over a distance of approximately 8mm from the top of the cavity in order to avoid large discontinuities in the solute concentration field, and provide more realistic field comparisons as step transitions were not found to occur naturally [6].

CFL Stability

The time step was varied throughout the simulation to maintain the maximum CFL number in the range of 0.35-0.45 [9], where $0.35 < \text{CFL} = \Delta t u_i / \Delta x_i < 0.45$.

Ramp Inlet Boundary Conditions

In order to vary the time to start-up, ramp inlet boundary conditions have been used. In each case, the inlet velocity increases linearly with the simulation time until the ramp time is reached, and then the velocity is held constant for the remainder of the simulation. Ramp times varied from an instantaneous start-up to 7 minutes, the latter bound was chosen as it was found the splash didn't vary significantly for start-up times longer than this.

Results

The simulations are integrated until the interface crosses the outlet edge (RHS) of the cavity, indicating the end of the initial splash. Each simulation is monitored for both the area (or volume) of saline liquid purged out of the cavity and the maximum drop in the interface height. As the interface diffuses to different extents for different ramp times, both the area and interface height are given for a volume fraction of 0 (fresh), 0.5 and 1 (salty). This provides the minimum and maximum possible bounds of saline liquid purged for each simulation. The volume of fluid purged from the cavity is calculated by integrating the non-dimensional solute concentration isolines.

The initial splash is considered to be effective if the splash contains non-diffused saline liquid, i.e. water with a density equal to that initially in the cavity. Using this definition, the last effective splash occurs for a ramp start-up of 15 seconds, as by 20 seconds the initial splash contains only the liquid in the originally diffused interface. Figure 2 contains the area of saline liquid purged from the cavity with a non-dimensional solute concentration of 1.0 plotted against the dimensional simulation time. As the ramp-time is increased, the time for the splash to begin is also increased. For all efficient ramp start-up times, the effective splash finished by 4.5 seconds. The profile of the splash also changes as the ramp time is increased, with the amplitude of the splash decreasing with increasing ramp times.

The start-up time of 3 seconds is the most effective of all the ramp times examined in this paper according to the above definition, however the total volume of saline liquid purged when accounting for the diffused fluid is the largest for the

instantaneous start-up. Figure 3 depicts the maximum volume of saline fluid purged from the cavity. The maximum volume of saline liquid purged is calculated by finding the area under the isoline for a non-dimensional solute concentration of 0.01, which represents the top of the interface. As the start-up time is increased from an instantaneous start, the total volume of saline fluid purged out of the cavity is decreased.

Immediately after the simulation start-up, the interface tilts with the highest point at the downstream wall of the cavity. The tilt in the interface level is proportional to the ramp start-up time, where the fastest start-up will have the largest interface tilt. The initial splash is largest for cases where this interface is capable of tilting the most, as the tilt exceeds the height of the cavity wall, and the dense saline liquid is advected away with the overflow once the interface has tilted above the level of the downstream cavity wall. In long start-up times, the interface tilts only enough to present the diffused interface to the fresh overflowing water, and hence only the diffused interface is advected away by the overflow. For ramp times sufficiently long, the interface initially tilts, however it has not been lifted high enough to pass out of the cavity, and hence falls back into the cavity and creates oscillations on the interface, which grow as the simulation progresses. Thus, for start-up times longer than 15 seconds, Stage 1 of the purging process is suppressed.

Stage 2 reported in [2], where the vorticity generated at the upstream corner of the cavity forms a vortex with an accompanying second splash, has the strongest formed vortex for the instantaneous case. The strength of this vortex decreases with increasing ramp time. For ramp times of 15 seconds and longer, the vorticity is not strong enough to promote the growth of the vortex, and hence the second splash does not occur for these cases. Thus stage 2 of the purging process is suppressed for ramp times of 15 seconds and longer.

As the ramp start-up time is increased above 30 seconds, the diffused interface is the only saline liquid purged out of the cavity in the initial splash, and once this has been purged, the interface becomes one of a step transition, where the buoyancy forces are stronger. The interface then begins to oscillate, increasing in amplitude as the simulation continues. As the interface oscillates, if the amplitude of the oscillation is higher than the downstream corner of the cavity, diffused saline fluid is passed out of the cavity and carried away by the overflow. This is indicative of Stage 3 in the instantaneous start-up case, which is apparent for all ramp start-up times. Thus, for long ramp times, the transport of the fluid out of the cavity is driven by oscillations on the interface within the cavity, which grow as the simulation progresses, and the purging is characterised by a series of small diffused liquid splashes rather than one significant splash.

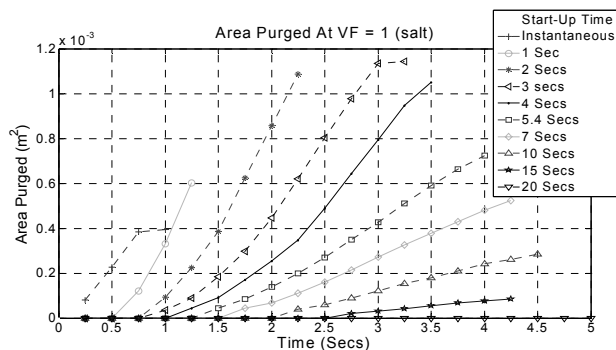


Figure 2. Area of Saline Liquid purged from cavity with non-dimensional solute concentration of 1 for “effective” purging ramp times.

The interface height therefore drops slowly for long start-up times compared to the instantaneous start-up. If the start-up time is increased to 7 minutes, the oscillation allows fluid to pass out both of the upstream and downstream end of the cavity. Once the velocity in the channel increases sufficiently, the fluid purged out of the upstream end of the cavity is washed back into the cavity.

Drop in Interface Height Trends

The drop in the interface level at the end of the initial splash is plotted against the ramp start-up time in Figure 4. As the ramp start-up time is increased from an instantaneous start-up, the maximum drop in the interface height from its initial position decreases, and for ramp start-up times longer than 60 seconds, the height of the interface is not significantly lowered from its original position. It is concluded that for ramp times longer than 60 seconds, the initial surge wave is completely suppressed, and the transport of saline liquid out of the cavity is dominated by the oscillations of the interface, which periodically forces diffused liquid out of the cavity in a series of small splashes. The period of the oscillation is approximated by the cavity scale seiche.

The Seiche Frequency

The oscillations on the interface described above for cases with long start-up times have an approximate period of the first mode of the internal seiche, given by [13]:

$$P = \lambda \left[\frac{\Delta \rho g}{k} (\rho_s \coth kh_{cav} + \rho_f \coth kh_{chan})^{-1} \right]^{-1/2} \quad (12)$$

where $k = \pi / (h_{cav} n)$; and the wavelength, $\lambda = 2l/n$. Here n is the mode number, g the gravity; $\Delta \rho = \rho_s - \rho_f$; and l is the length of the cavity. For this case, the period of the first mode of oscillation is 7.11 seconds, and the period of the second mode is 5.02 seconds.

By monitoring the oscillation of the interface ($VF = 0.1$) at a distance of 0.006 m from the left hand side of the cavity, the first mode of oscillation of the internal seiche is clearly seen for long ramp start-up times, i.e. 60 seconds and longer. The average period of oscillation of the interface for different ramp times included in Table 1.

Ramp-Time	Sample Time	Average Period of Oscillation
1 minute	0-20.5 secs	7.354 secs
1.5 minutes	0-30 secs	6.719 secs
2 minutes	0-70 secs	5.975 secs
3 minutes	0-140 secs	6.950 secs
5 minutes	0-160 secs	6.627 secs

Table 1. Average period of oscillation of the interface at a distance of 0.006m in from the LHS of the cavity, with solute concentration 0.1.

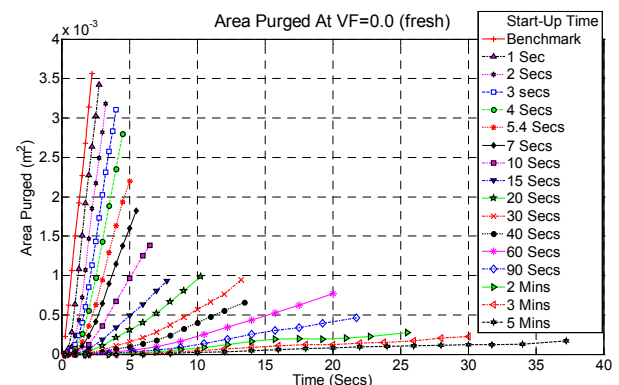


Figure 3. Area of Saline Liquid purged from cavity calculated from non-dimensional solute concentration isoline 0.01 for all purging ramp times.

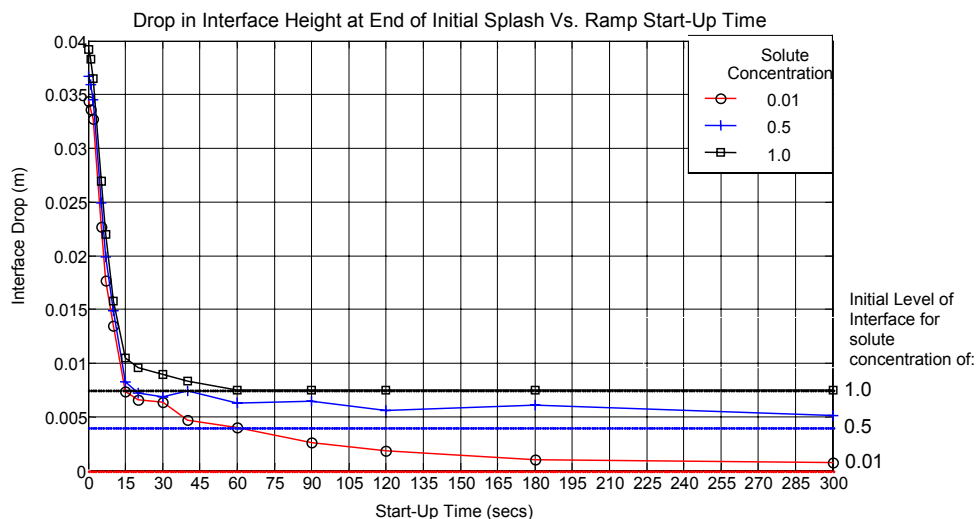


Figure 4. Drop in the height of the interface from the top of the cavity at the end of the initial splash plotted against the ramp time. For ramp times of 60 seconds and longer, the interface with a non-dimensional solute concentration of 1 has not moved from its original position.

The oscillation begins at 5.75 seconds for ramp times longer than the first mode period of 7.11 seconds (i.e. 10 secs and longer), and all simulations have an obvious response in the level of the interface (drops momentarily) at this time. As each simulation was monitored every 0.25 seconds, information between these time-steps is not known, and hence the error in this period is of the order of 0.25 secs. The oscillations increase in amplitude until a point in the simulation, after which the period of the oscillation decreases. At this point, a wave begins to travel across the interface from left to right, depressing the interface on the right hand side of the cavity and which responds with waves of increasing amplitude in this region. The mode of oscillation during this time is better approximated by the second mode seiche. The interface then sloshes back and forth, enabling the transport of fluid out of the cavity as the wave surges into the right side cavity wall.

Plotting the height of the interface based on a non-dimensional solute concentration of 0.1 for the 5 minute ramp start-up (Figure 5), the period of the first mode of the seiche is constant from 26 seconds with a period of 6.75 seconds. This first mode seiche frequency promotes the transport of the diffused saline fluid out of the cavity, as the amplitude of the oscillation increases with time, which results in the periodic splashing of diffused fluid out of the cavity.

For the long start-up times examined in this case, the oscillation of the first mode of the cavity scale seiche drives the transport of diffused saline liquid out of the cavity. Ramp start-up times equal to the first and second modes of the seiche were simulated, however the volume of purged saline liquid and the drop in the interface height did not deviate from the trends obvious from the adjacent results. However, an interesting feature discovered is that for ramp times less than the period of the first mode of the seiche, the initial splash finishes after the specified ramp time, whereas for ramp times longer than the seiche period, the splash finishes before the ramp time. Thus, although using the first mode seiche period as the ramp time will not increase the purging rate of the cavity, the time for the initial splash to pass will be known. This may have benefits when running pulsating flows, i.e. where the flow is ramped up and down periodically.

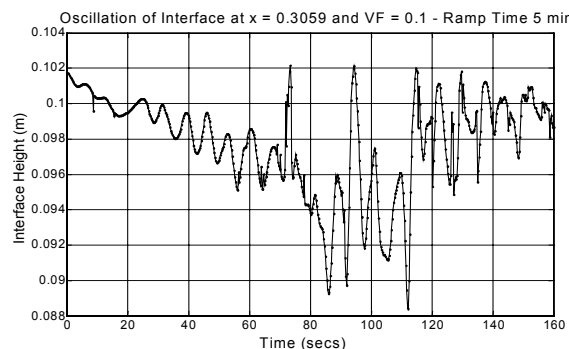


Figure 5. Plot of the interface monitored at 0.006 in from the left hand side wall of the cavity with solute concentration equal to 0.1 for 5 minutes to start-up.

Conclusions

By removing the instantaneous start-up of the simulation, the first 2 stages of the purging process for instantaneous start-ups may be suppressed, i.e. the initial wave and shed vortex. In general, suppression of these stages occurs for long start-up times.

This is of concern to catchment management who need to maximise the purging of the pools while minimising the volume of water released in order to purge the pool. When the initial splash is suppressed, it is replaced by a slow erosion of the saline interface, with oscillations on the interface periodically forcing out small volumes of diffused interface into the overflow. The period of these oscillations is approximately equal to the first mode seiche frequency of the cavity.

Although shorter ramp times splash larger quantities of dense saline liquid out of the cavity in a relatively short time, a fast release regime into a river may not only be unfeasible, but it could result in the poisoning of other deeper areas downstream. If the saline fluid purged from the cavity does not diffuse into the overflow, the purged fluid will most likely travel along the base of the river until the flow ceases. Also, care must be taken not to increase the salinity of the overflowing water above total dissolved solids concentrations set in individual catchments.

Acknowledgments

The first author would like to thank the Wimmera Catchment Management Authority in Horsham, Victoria, for access to field data. This research is supported by the Australian Research Council in the form of an Joint ARC Linkage project (LP0562390) undertaken with the Victorian Environmental Protection Authority, The University of Sydney and Griffith University.

References

[1] J.R.Anderson & A.K.Morison, "Environmental Consequences of Saline Groundwater Intrusion into the Wimmera River, Victoria", BMR J. Aust. Geol. Geophysics., **11**, 1989, 233-235.

[2] S.W.Armfield & W.Debler, "Purging of Density Stabilised Basins", Int J Heat Mass Transfer, **36** No 2, 1993, 519-530.

[3] S.W.Armfield & R.Street, "The fractional-step method for the Navier-Stokes equations on staggered grids", Int. J. Numer. Meth. Fluids, **38**, 2002, 255-285.

[4] P.G.Cook, F.W.Leaney, I.D.Jolly, "Groundwater Recharge in the Mallee Region, and salinity implications for the Murray River – A Review", Prepared for the Murray Mallee Local Action Planning Association Inc, CSIRO Land and Water, Technical Report 45/01, November 2001.

[5] W.Debler & S.W.Armfield, "The purging of saline water from rectangular and trapezoidal cavities by an overflow of turbulent sweet water", J. Hydr. Res., **35**, No.1, 1997, 43-62.

[6] W.Debler & J.Imberger, "Flushing Criteria in Estuarine and Laboratory Experiments", J. Hydraul. Eng., **122**, No.12, 1996, 728-734.

[7] F.Dyer, R.Carter & T.Robson, "Environmental Flows: Report on the 2004/2005 releases in the Wimmera and MacKenzie Rivers", August 2005, Wimmera Catchment Management Authority, (www.wcma.vic.gov.au)

[8] O.B.Fringer, S.W.Armfield and R.L.Street, "Reducing numerical diffusion in interfacial gravity wave simulations", Int J Numer. Meth. Fluids, **39**, 2005, 301-329

[9] M.P.Kirkpatrick & S.W. Armfield, "Experimental and large eddy simulation results for the purging of salt water from a cavity by an overflow of fresh water", International Journal of Heat and Mass Transfer, **48**, 2005, 341-359

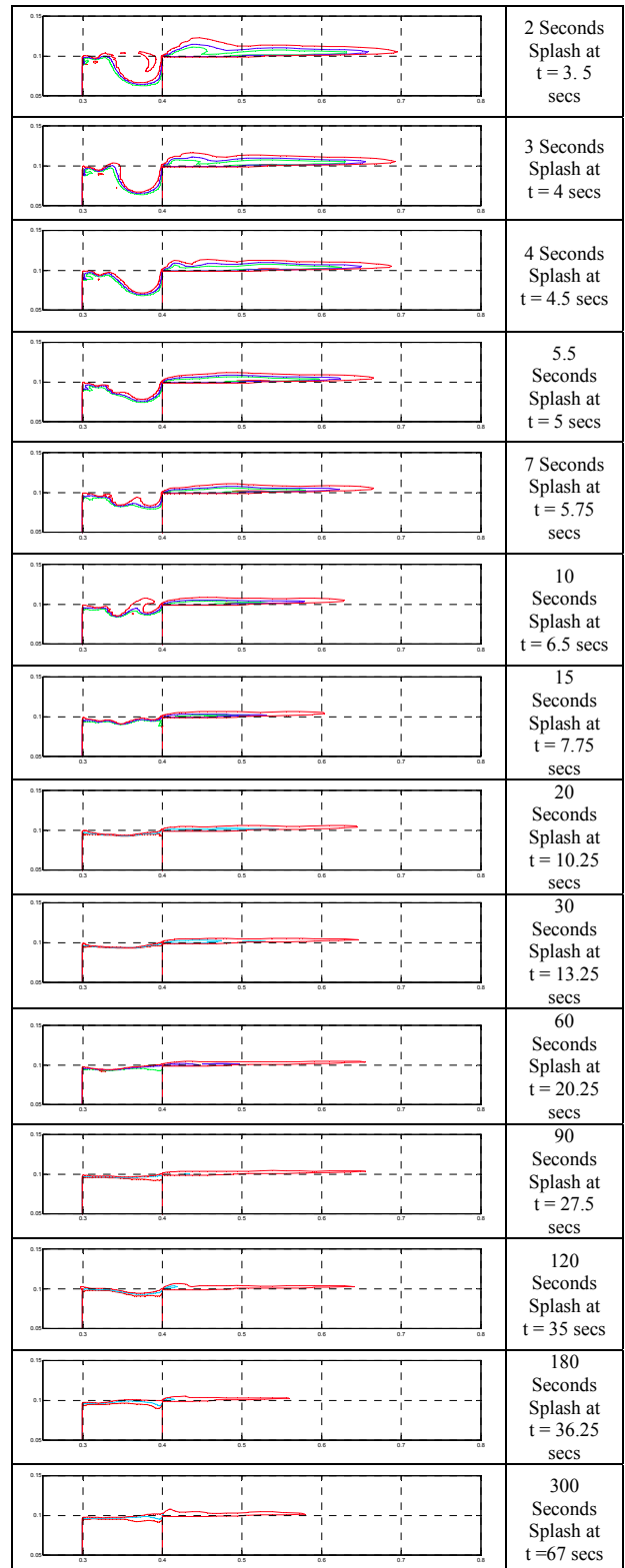
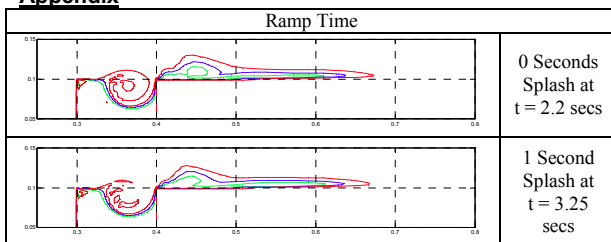
[10] B.P. Leonard, "A Stable and Accurate Convective Modelling Procedure Based on Quadratic Upstream Interpolation", Computational Methods in Applied Mechanical Eng., **19**, 1979, 59-98

[11] B.P.Leonard 'Simple High-Accuracy Resolution Program for Convective Modelling of Discontinuities', Int. J. Numer. Meth. Fluids, **8**, 1988, 1291-1318

[12] A.J.Peck & D.R.Williamson, "Effects of forest clearing on groundwater", J.Hydrol., **94**, 1987, 47-65

[13] S.Turner, "Buoyancy Effects in Fluids", Cambridge University Press, Cambridge, 1979

Appendix



Profiles of the initial splash for investigated ramp times.